

1
1 **AIR POLLUTION OVER NORTH-WEST BAY OF**
2 **BENGAL IN THE EARLY POST-MONSOON SEASON**
3 **BASED ON NASA MERRAERO DATA**

4

5 Pavel Kishcha,

6 *Department of Geophysical, Atmospheric and Planetary Sciences, Tel-Aviv University,*

7 *69978 Tel-Aviv, Israel*

8

9 Arlindo M. da Silva

10 *Global Modeling and Assimilation Office, NASA/GSFC, Greenbelt, Maryland USA.*

11

12 Boris Starobinets

13 *Department of Geophysical, Atmospheric and Planetary Sciences, Tel-Aviv University,*

14 *69978 Tel-Aviv, Israel*

15

16 Pinhas Alpert

17 *Department of Geophysical, Atmospheric and Planetary Sciences, Tel-Aviv University,*

18 *69978 Tel-Aviv, Israel*

19

20 Journal of Geophysical Research – Atmospheres,

21

Submitted in June 2013

2

22Abstract

23The MERRA Aerosol Reanalysis (MERRAero) has been recently developed at NASA's
24Global Modeling Assimilation Office (GMAO). This reanalysis is based on a version of
25the GEOS-5 model radiatively coupled with GOCART aerosols, and it includes
26assimilation of bias-corrected Aerosol Optical Thickness (AOT) from the MODIS
27sensor on both Terra and Aqua satellites. Our main finding is that, in October, in the
28absence of aerosol sources in north-west Bay of Bengal (BoB), MERRAero showed
29increasing AOT trends over north-west BoB exceeding those over the east of the
30Ganges basin. The Ganges basin is characterized by significant population growth
31accompanied by developing industry, agriculture, and increasing transportation: this has
32resulted in declining air quality. MERRAero data for the period 2002-2009 was used to
33study AOT trends over north-west Bay of Bengal (BoB) in the early post-monsoon
34season. This season is characterized by aerosol transport from the Ganges basin to
35north-west BoB by prevailing winds; and still significant rainfall of over 150
36mm/month. Different aerosol components showed strong increasing AOT trends over
37north-west BoB. The following factors contributed to the increasing AOT trend over the
38area in question in October: an increasing number of days when prevailing winds blew
39from land to sea, resulting in a drier environment and an increase in air pollution over
40north-west BoB; wind convergence was observed over north-west BoB causing the
41accumulation of aerosol particles over that region, when prevailing winds blew from
42land to sea. MERRAero aerosol reanalysis can be used on a global scale.

43

44

45

461. Introduction

47The Indian subcontinent (and the Ganges basin in particular) is characterized by a
48significant population growth accompanied by developing industry, agriculture, and
49increasing transportation. This has resulted in declining air quality [Di Girolamo et al.
502004, Ramanathan and Ramana, 2005, Tripathi et al., 2005, Prasad and Singh, 2007,
51Kaskaoutis et al., 2011a, Dey and Di Girolamo, 2011, Krishna Moorthy et al., 2013].
52With respect to air pollution, one could suggest some relationship between population
53figures and anthropogenic aerosol emissions. Indeed, Kishcha et al. [2011] showed that,
54over extensive areas with differing population densities in the Indian subcontinent, the
55higher the averaged population density – the larger the averaged AOT. In addition, the
56larger the population growth - the stronger the increasing AOT trends.

57

58Prevailing winds blowing along the Ganges basin in the post-monsoon and winter
59months transport anthropogenic aerosol particles into the Bay of Bengal (BoB) [Di
60Girolamo et al. 2004, Prasad and Singh, 2007, Kumar et al., 2010]. The resulting
61increased levels of air pollution over BoB were investigated during a number of sea
62expeditions [Ramachandran and Jayaraman, 2003; Vinoj et al., 2004; Ganguly et al.,
632005, Moorthy et al., 2008, Kumar et al., 2010, Kaskaoutis et al., 2011b]. Moreover,
64long-term AOT trends over South Asia, including BoB, were examined, using different
65satellite AOT data sets, by Mishchenko and Geogdzhayev [2007], Zhao et al. [2008],
66Zhang and Reid [2010], Kaskaoutis et al. [2011a], Dey and Di Girolamo [2011], and
67Hsu et al. [2012]. Based on AVHRR satellite data, Mishchenko and Geogdzhayev
68[2007] compared over-water AOT averaged over two separate periods, 1988–1991 and
692002–2005, and found significant changes. Zhao et al. [2008] studied AOT trends over
70the whole area of BoB for spring, summer, autumn, and winter during the 25-year
71period 1981 – 2005, using AVHRR data. Using MODIS-Terra Level 2 AOT data,
72Zhang and Reid [2010] analyzed AOT trends over the whole area of BoB for all months
73during the 10-year period 2000 - 2009. The spatial distribution of decadal (2000 – 2009)
74MODIS Level-3 AOT trends over South Asia, including BoB, in different months was
75obtained by Kaskaoutis et al. [2011a]. Using MISR aerosol data, decadal (2000 – 2009)
76AOT trends over the Indian subcontinent and surrounding sea areas were also estimated
77by Dey and Di Girolamo [2011]. Hsu et al. [2012] created maps of SeaWiFS AOT
78trends over the period 1998 – 2010 for each of the four seasons. In the aforementioned

79studies, however, specific features of AOT trends over north-west BoB in the early
80post-monsoon season were not discussed.

81

82The early post-monsoon season over the study region is characterized by aerosol
83transport from the Ganges basin to north-west BoB by prevailing winds; and still
84significant rainfall of over 150 mm/month over the east of the Ganges basin and north-
85west BoB. It would be reasonable to consider that AOT trends over sea areas in BoB
86were created by changes in aerosol sources on the land in the Indian subcontinent. In
87our previous study [Kishcha et al., 2012], we found that it was not always the case.
88Specifically, we found that, in October, MODIS showed strong increasing aerosol
89optical thickness (AOT) trends over north-west Bay of Bengal (BoB) in the absence of
90AOT trends over the east of the Indian subcontinent. This was unexpected, because
91sources of anthropogenic pollution were located over the Indian subcontinent, mainly in
92the Ganges basin, and aerosol transport from the Indian subcontinent to north-west BoB
93was carried out by prevailing winds.

94

95It was interesting to determine whether existing state-of-the-art aerosol data-assimilated
96systems were capable of reproducing the aforementioned observed AOT trends over
97north-west BoB, in the early post-monsoon season, in the presence of significant
98rainfall. For the model, it would be a challenge just to obtain correct space-time
99distribution of rainfall, which is of importance for estimating aerosol wet removal. The
100NASA Goddard Earth Observing System (GEOS-5) was used to extend the NASA
101Modern Era-Retrospective Analysis for Research and Applications (MERRA)
102reanalysis by adding five atmospheric aerosol components (sulfates, organic carbon,
103black carbon, desert dust, and sea-salt). In the current study, the obtained eight-year
104(2002 – 2009) assimilated aerosol dataset (so-called MERRAero) was applied to
105examine aerosol trends over north-west Bay of Bengal (BoB) in the post-monsoon
106season. Using an assimilated aerosol dataset over north-west BoB provided us with an
107opportunity to estimate the contribution of different aerosol components to AOT and its
108trends. It is worth noting that only AOT was assimilated by GEOS-5, while details of
109the aerosol specification are to a large extent dependent on emission inventories assumed
110by the model.

111

1122. GEOS-5 and the MERRA Aerosol Reanalysis (MERRAero)

113

1142.1 GEOS-5 Earth Modeling System

115GEOS-5 is the latest version of the NASA Global Modeling and Assimilation Office
116(GMAO) Earth system model. GEOS-5 contains components for atmospheric
117circulation and composition (including atmospheric data assimilation), ocean circulation
118and biogeochemistry, and land surface processes. Components and individual
119parameterizations within components are coupled under the Earth System Modeling
120Framework (ESMF) [Hill et al., 2004]. In addition to traditional meteorological
121parameters (winds, temperatures, etc. [Rienecker et al., 2008]), GEOS-5 includes
122modules representing the atmospheric composition, most notably aerosols [Colarco et
123al., 2010], and tropospheric/stratospheric chemical constituents [Pawson et al., 2008],
124and the impact of these constituents on the radiative processes of the atmosphere.

125

1262.2 Aerosols in GEOS-5

127GEOS-5 includes modules representing atmospheric composition, including aerosols
128[Colarco et al., 2010] and tropospheric and stratospheric chemical constituents [Pawson
129et al., 2008]. The current generation aerosol module is based on a version of the
130Goddard Chemistry, Aerosol, Radiation, and Transport (GOCART) model [Chin et al.,
1312002]. GOCART treats the sources, sinks, and chemistry of dust, sulfate, sea salt, and
132black and organic carbon aerosols. Aerosol species are assumed to be external mixtures.
133Aerosol emissions are based on the AeroCom version 2 hindcast inventories [Dr.
134Thomas Diehl, personal communication, and <http://aerocom.met.no/emissions.html>].
135Total mass of sulfate and carbonaceous aerosols are tracked, while for dust and sea salt
136the particle size distribution is explicitly resolved across five non-interacting size bins
137for each. Both dust and sea salt have wind-speed dependent emission functions, while
138sulfate and carbonaceous species have emissions principally from fossil fuel
139combustion, biomass burning, and bio-fuel consumption, with additional biogenic
140sources of organic carbon. Sulfate has additional chemical production from oxidation of
141SO₂ and dimethylsulfide (DMS), as well as a database of volcanic SO₂ emissions and
142injection heights.

143

144For all aerosol species, optical properties are primarily from the commonly used Optical
145Properties of Aerosols and Clouds (OPAC) data set [Hess et al., 1998]. OPAC provides
146the spectrally varying refractive index and a humidification factor for each aerosol
147species which, together with assumptions about the particle size distribution of each
148species, are used to construct spectrally varying lookup tables of aerosol optical
149properties such as the mass extinction efficiency, single scattering albedo, and
150asymmetry parameter, inputs required by our radiative transfer codes (details are in
151Colarco et al. [2010], and references therein). Daily biomass burning emissions are from
152the Quick Fire Emission Dataset (QFED) and are derived from MODIS fire radiative
153power retrievals [Darmenov and da Silva, 2013].

154

1552.3 GEOS-5 Data Assimilation

156GEOS-5 has a mature atmospheric data assimilation system that builds upon the Grid-
157point Statistical Interpolation (GSI) algorithm, jointly developed with NCEP [Wu et al.
1582002, Derber et al. 2003, Rienecker et al. 2008]. The GSI solver was originally
159developed at NCEP as an unified 3D-Var analysis system for supporting global and
160regional models. GSI includes all the in-situ and remotely sensed data used for
161operational weather prediction at NCEP.

162GEOS-5 also includes assimilation of AOT observations from the MODIS sensor on
163both Terra and Aqua satellites. Based on the work of Zhang and Reid [2006] and Lary
164[2009], a back-propagation neural network has been developed to correct observational
165biases related to cloud contamination, surface parameterization, aerosol microphysics,
166etc. On-line quality control is performed with the adaptive buddy check of Dee et al.
167[2001], with observation and background errors estimated using the maximum
168likelihood approach of Dee and da Silva [1999]. The AOT analysis in GEOS-5 is
169performed by means of analysis splitting. First, a 2D analysis of AOT is performed
170using error covariances, derived from innovation data. The 3D analysis increments of
171aerosol mass concentration are computed using an ensemble formulation for the
172background error covariance. In MERRAero, as well as in the GEOS-5 near real-time
173system, this calculation is performed using the Local Displacement Ensemble (LDE)
174methodology under the assumption that ensemble perturbations are meant to represent

175misplacements of the aerosol plumes. These ensemble perturbations are generated with
176full model resolution, without the need for multiple model runs.

177

1782.4 MERRA Aerosol (MERRAero) Reanalysis

179MERRA is a NASA reanalysis for the satellite era using a major new version of the
180Goddard Earth Observing System Data Assimilation System Version 5 (GEOS-5). The
181Project focuses on historical analyses of the hydrological cycle from the NASA EOS
182suite of observations in a climate context, on a broad range of weather and climate time
183scales and places. The MERRA time period covers the modern era of remotely sensed
184data, from 1979 through the present, and the special focus of the atmospheric
185assimilation is the hydrological cycle. Like other similar reanalysis, MERRA provides
186meteorological parameters (winds, temperature, humidity), along with a number of
187other diagnostics such as surface and top of the atmosphere fluxes, diabatic terms and
188the observational corrections imposed by the data assimilation procedure.

189As a step toward an Integrated Earth System Analysis (IESA), the GMAO is producing
190several parallel re-analyses of other components of the earth system such as ocean, land
191and atmospheric composition. Of particular relevance for this paper the MERRA Aerosol
192Reanalysis (MERRAero), where MODIS AOT observations are assimilated providing a
193companion aerosol gridded datasets that can be used to study the impact of aerosols on
194the atmospheric circulation and on air quality in general. Table 1 summarizes the main
195attributes of MERRAero. Notice that MERRAero only covers the later years of
196MERRA, capitalizing on the improved aerosol measurements from NASA's EOS
197platforms.

198

1993. Method

200Following our previous study [Kishcha et al., 2012], we analyzed long-term variations
201of AOT over seven zones, each $3^\circ \times 3^\circ$, located in the Ganges basin and north-west BoB
202(Fig. 1). As mentioned, in the post-monsoon period, prevailing winds blow along the
203Ganges basin. The specified zones in the Ganges basin provide us with an opportunity
204for analyzing air pollution trends produced by local sources and aerosol transport. Fig.
2051a shows the spatial distribution of eight-year mean MERRAero AOT over the region
206under consideration in October, together with the location of zones $3^\circ \times 3^\circ$ in the Indian

207subcontinent (zone 1 to zone 5) and in the Bay of Bengal (zones 6 and 7). MERRAero
208monthly AOT data are available from the year 2002. To analyze AOT and its trends
209over the Indian subcontinent and north-west BoB, we used monthly MERRAero AOT
210data with horizontal resolution of approximately 50 km, during the eight-year period
2112002 – 2009.

212

213A linear fit was used to determine the resulting trend of aerosol optical thickness during
214the study period (2002 – 2009) over each of the aforementioned zones. The obtained
215AOT trend values correspond to the slope of the linear fit. To ensure that the linear fit
216produced normally distributed residuals, they were required to pass the Shapiro–Wilk
217normality test [Shapiro and [Wilk](#), 1965, Razali and Wah, 2011]. If the residuals were
218normally distributed, they could be used in a t-test, in order to estimate the statistical
219significance of a linear fit. The statistical significance of the AOT trend was checked by
220applying the significance level (p) value, i.e. $p < 0.05$ for statistically significant AOT
221trends at the 95 % confidence level.

222

2234. Results

2244.1. Comparison between total MERRAero and MODIS AOT trends in October

225In accordance with space distribution of eight-year mean AOT in the early post-
226monsoon season (October), MERRAero showed high AOT values over the Ganges
227basin with a maximum over the north-west part of the Ganges basin (Fig. 1a).
228Therefore, MERRAero data were able to reproduce the main structure of aerosol
229distribution over the Ganges basin. The Ganges basin is the most polluted part of the
230Indian subcontinent, where highly-populated areas and main industrial centers are
231located.

232

233We analyzed zone-to-zone variations of MERRAero AOT averaged over the specified
234zones. In the early post-monsoon season (October), MERRAero showed mainly
235decreasing AOT variations from zone 3 to zone 5 (Fig. 2a and Table 2). Note that this
236decrease in AOT from north-west to east of the Ganges basin does not correspond to the
237distribution of population density: population density is higher in the east of the Ganges
238basin (zones 4 and 5) than in the north-west of the Ganges basin (zone 1) (Fig. 3). At

239first glance, this is contradictory to our previous findings on the relationship between
240AOT and population density in the Indian subcontinent [Kishcha et al., 2011]. It should
241be mentioned, however, that, in our previous study, we used averaging over significant
242areas of the Indian subcontinent with differing population densities.

243

244The most probable reason for the decrease in AOT over the east of the Ganges basin,
245where population density is the highest in the Ganges basin, is wet removal processes
246after significant rainfall in October. Monthly accumulated Tropical Rainfall Measuring
247Mission (TRMM) rainfall data from the 3B42V6 archive, on a $0.25^\circ \times 0.25^\circ$ latitude-
248longitude grid [Huffman et al., 2007], were used to estimate zone-to-zone variations of
249eight-year (2002 – 2009) mean TRMM rainfall over the specified zones in October (Fig.
2504). High rainfall values of over 150 mm can be seen in October over the east of the
251Ganges basin (zone 5) and north-west BoB (zone 6). Moreover, rainfall data showed
252that, over the east of the Ganges basin, the accumulated rainfall in October in the first
253four-year period 2002 – 2005 was essentially higher than in the second four-year period
2542006 – 2009 (Fig. 4). As a result, higher values of MERRAero AOT over the east of the
255Ganges basin (zones 4 and 5) were observed in the second four-year period 2006 – 2009
256than in the first four-year period 2002 – 2005 (Fig. 2b).

257

258Space distributions of MERRAero AOT trends during the eight-year (2002 – 2009)
259study period showed strong increasing AOT trends over north-west BoB exceeding
260those over the Ganges basin (Fig. 1b). This indicates that MERRAero is capable of
261reproducing the main features of the phenomenon of strong increasing AOT trends over
262north-west BoB in the early post-monsoon season, in line with our previous study
263[Kishcha et al., 2012].

264

2654.2. Effects of rainfall on MERRAero AOT

266As mentioned, in the early post-monsoon season (October), intense rainfall can be
267frequently observed over the east of the Ganges basin. These severe precipitation events
268could strongly affect AOT over the east of the Ganges basin due to aerosol wet removal
269processes. To understand the rain effects on AOT over the east of the Ganges basin
270(zone 5), we compared year-to-year variations of assimilated MERRAero AOT and
271TRMM accumulated rainfall, over zone 5 in each October during the study period (Fig.
2725a). Rainfall data showed that the accumulated rainfall in October in the first four-year

273 period 2002-2005 was higher than in the second four-year period 2006-2009 (Fig. 5a).
 274 A strong inverse negative relationship (with a high negative correlation of over -0.8)
 275 between changes in assimilated MERRAero AOT and rainfall is clearly seen: each
 276 increase in rainfall was accompanied by a decrease in assimilated AOT (Fig. 5a). The
 277 aforementioned decrease in rainfall over zone 5 in October during the study period can
 278 explain some increasing trend in MERRAero AOT observed over that area in October
 279 (Fig. 5a and Table 2). There was some dissimilarity in the rainfall amount between the
 280 east of the Ganges basin (zone 5) and north-west BoB (zone 6): Fig. 5b does not show
 281 as clear decreasing trends in rainfall amount over north-west BoB as over the east of the
 282 Ganges basin in Fig. 5a.

283

284 4.3. AOT of different aerosol species and their trends in the early post-monsoon 285 season

286 As known, satellite remote sensing data can not distinguish between different aerosol
 287 species. MERRAero provides us with an opportunity to investigate the contribution of
 288 different aerosol components to AOT and its trends. Based on MERRAero model data,
 289 Fig. 6a represents zone-to-zone variations of eight-year (2002 – 2009) mean AOT of
 290 several aerosol components (desert dust; organic and black carbon; and sulfates)
 291 averaged over specified zones in October, and their trends. One can see that, over zone
 292 1, there was a considerable amount of carbon aerosols (as a result of crop waste burning
 293 [Sharma et al., 2010]), dust particles, and sulfate aerosols (Fig. 6a). This explains the
 294 AOT maximum over the north-west of the Ganges basin in October.

295

296 By contrast to sulfates and carbonates, dust aerosol particles have no sources along the
 297 Ganges basin. Therefore, dust distribution along the Ganges basin is determined by
 298 aerosol transport (by the action of prevailing winds blowing along the Ganges basin)
 299 and by deposition processes. One can see that the eight-year mean dust AOT values
 300 noticeably decreased along the Ganges basin and over north-west BoB. This resulted in
 301 the decrease in dust contribution to the total AOT from approximately 30% over zone 1
 302 to 8% over zones from 5 to 7 (Table 3). Furthermore, dust AOT trends did not change in
 303 transition from land to sea: approximately the same slightly increasing dust AOT trends
 304 of $\sim 0.004 \text{ yr}^{-1}$ were obtained along the east of the Ganges basin and over north-west
 305 BoB (Fig. 6b). We found that these AOT trends over zones from 5 to 7 were statistically
 306 significant (Table 3). The same dust AOT trends along the Ganges basin and over north-

307west BoB suggest an increasing trend in some external source of dust emissions, outside
308the Ganges basin. It should be kept in mind that MERRAero only assimilates total AOT
309and that the trend in aerosol speciation may depend on the trend (or lack thereof) of the
310specified emissions.

311

312The distribution of sulfate AOT along the Ganges basin is determined by sulfate aerosol
313emissions, together with aerosol transport (by the action of prevailing winds) and
314deposition processes (Fig. 6a). The sulfate contribution to the total AOT increased along
315the Ganges basin from approximately 30 % over zone 1 to ~56% over zone 5 (Table 3).
316Over north-west BoB (zones 6 and 7), the sulfate contribution to the total AOT was
317over 50% (Table 3). Thus, according to MERRAero AOT data, sulfates were the major
318atmospheric aerosol component over the east of the Ganges basin and over north-west
319BoB. Moreover, MERRAero data showed that sulfate AOT trends changed in transition
320from land to sea: strong statistically-significant increasing sulfate AOT trends (of 0.008
321 yr^{-1} and 0.011 yr^{-1} over zones 6 and 7 respectively) exceeded those over the east of the
322Ganges basin (zone 5) (Fig. 6b, and Table 3).

323

324With respect to organic and black carbon aerosols, their distribution of eight-year mean
325AOT values along the Ganges showed a wide maximum from the north-west to the
326center of the Ganges basin (zones from 1 to 3) (Fig. 6a). This area of maximum carbon
327AOT is known for crop waste burning aerosols [Sharma et al., 2010. Venkataraman et
328al., 2006]. AOT values of carbon aerosols decrease to the east from zone 3 (Fig. 6a). As
329discussed in Section 4.1, the reason for the decrease in AOT over the east of the Ganges
330basin in October is significant rainfall accompanied by aerosol wet removal processes.
331The joint contribution of organic and black carbon aerosols to the total AOT is ~38%
332over the north-west of the Ganges basin (zones from 1 to 3); ~35% over the east of the
333Ganges basin (zone 5), and approximately 27% over north-west BoB (zones 6 and 7)
334(Table 3). Similar to AOT trends of sulfate aerosols, MERRAero showed that AOT
335trends of carbon aerosols changed in transition from land to sea: increasing AOT trends
336in organic and black carbon AOT over the sea (zones 6 and 7) exceeded those over zone
3375 in the land (Fig. 6b, and Table 3).

338

339Based on MERRAero data, we found that, in October, the contribution of sea-salt
340aerosols to the total AOT over the east of the Ganges basin and north-west BoB was

341 even lower than that of desert dust. Therefore, over the east of the Ganges basin and
342 north-west BoB in October, anthropogenic aerosols dominate natural aerosols (Table 3).
343

344 4.4. Factors contributing to AOT trends over north-west BoB

345 MERRAero showed increasing AOT trends over north-west BoB in October exceeding
346 AOT trends over the east of the Ganges basin (Fig. 1b). This was despite the fact that
347 sources of air pollution are located on the land, mainly in the Ganges basin. There could
348 be several factors contributing to the increasing AOT trends over north-west BoB. First,
349 there were changes in the atmospheric circulation over north-west BoB in October
350 during the eight-year study period (Fig. 7). Mean wind vectors of the 700-850 hPa layer
351 in each October during the 8-year period under consideration were analyzed (Fig. 7).
352 The 700-850 hPa layer is considered as indicative of wind in the lower troposphere,
353 where aerosol transport mainly occurs [Dunion and Velden, 2004]. During the second 4-
354 year period (2006 – 2009), prevailing winds blowing mainly from land to sea (Fig. 7, e -
355 h) resulted in a drier environment and less precipitation over the east of the Ganges
356 basin and north-west BoB (Fig. 4) than during the first 4-year period (2002 – 2005)
357 (Fig. 7, a - d). This caused less wet removal of air pollution in the second 4-year period
358 than in the first 4-year period. Second, our analysis showed that, during the eight-year
359 study period, there was an increasing number of days (N_p , in percentage form) in each
360 October when prevailing winds blew from land to sea (Fig. 8). This suggests some
361 increasing trends in the transport of anthropogenic air pollution from their sources in the
362 east of the Ganges basin to north-west BoB. Third, for Octobers when $N_p > 50\%$, wind
363 convergence was observed over north-west BoB causing the accumulation of aerosol
364 particles over that region (Fig. 9), in line with our previous study [Kishcha et al., 2012].
365 All the three factors contributed to the increasing AOT trend over north-west BoB in the
366 early post-monsoon season.

367

368 During the second 4-year period (2006 – 2009), a decrease in atmospheric humidity was
369 observed. We analyzed observations of atmospheric relative humidity from the AIRS
370 (Atmospheric Infrared Sounder) instrument aboard the NASA's Aqua satellite, available
371 from 2002 [Fasullo and Trenberth, 2012]. Fig. 10a represents year-to-year variations of
372 relative humidity (RH) of the 700-850 hPa layer over north-west BoB in each October
373 during the study period 2002 - 2009, taken on the ascending node of the Aqua satellite
374 orbit (on the day side of the Earth). Quite noticeable non-linear decreasing RH trends

375 can be clearly seen over north-west BoB (zones 6 and 7) during the study period.
 376 MERRA reanalysis (used as a driver for the GEOS-5 model in order to obtain
 377 MERRAero aerosol data set) was capable of reproducing the aforementioned observed
 378 changes in relative humidity over north-west BoB (Fig. 10b).

379

380 The aforementioned decrease in relative humidity over north-west BoB during the study
 381 period was accompanied by a decrease in the effective size of hygroscopic aerosol
 382 particles. This process contributed to a decrease in AOT of hygroscopic aerosols [Bian
 383 et al., 2009]. One could expect to get a direct relationship between AOT and RH: an
 384 increase in RH should lead to an increase in AOT. However, MERRAero showed an
 385 inverse relationship between AOT and RH: a decrease in RH over north-west BoB in
 386 October was accompanied by an increase in AOT (Fig. 11). This is evidence that other
 387 factors, affecting AOT, were more effective than the decrease in AOT due to the
 388 decrease in effective size of hygroscopic aerosol particles.

389

390 Consequently, there were competing processes affecting AOT over north-west BoB in
 391 the early post-monsoon season. MERRAero showed that these competing processes
 392 resulted in increasing AOT trends over north-west BoB exceeding those over the east of
 393 the Ganges basin.

394

395 5. Conclusions

396 The recently developed eight-year (2002 – 2009) MERRAero assimilated aerosol
 397 dataset was applied to the study of AOT and its trends over north-west BoB in the early
 398 post-monsoon season. Our main finding is that, in October, in the absence of aerosol
 399 sources in north-west BoB, MERRAero showed increasing AOT trends over north-west
 400 BoB exceeding those over the east of the Ganges basin. Different aerosol components
 401 showed strong increasing AOT trends over north-west BoB.

402

403 There were a number of factors contributing to the increasing AOT trend over the area
 404 in question:

- 405 • an increasing number of days in each October when prevailing winds blew from
 406 land to sea, resulting in an increase in air pollution over north-west BoB;

- 407 • during the second 4-year period (2006 – 2009), prevailing winds blowing mainly
408 from land to sea were responsible for a drier environment with less precipitation
409 causing less wet removal of air pollution than in the first 4-year period (2002 –
410 2005);
- 411 • in each October, when prevailing winds blew from land to sea, wind
412 convergence was observed over north-west BoB causing the accumulation of
413 aerosol particles over that region, in line with our previous study [Kishcha et al.,
414 2012].

415

416 Over the region under consideration, MERRAero showed the main structure of space
417 distribution of AOT in October, averaged over the study period: high AOT values over
418 the Ganges basin with a maximum over the north-west of the Ganges basin. The
419 MERRAero AOT data set allowed us to determine the causal factor for this AOT
420 maximum, which is a considerable amount of carbon aerosols (from bio-mass burning),
421 dust particles, and sulfates. Over north-west BoB in the early post-monsoon season,
422 MERRAero showed that aerosols were dominated by anthropogenic air pollution, such
423 as sulfates and carbon aerosols.

424 MERRAero aerosol reanalysis can be used on a global scale for analyzing AOT of
425 different aerosol species.

426

427References

- 428Bian, H., M. Chin, J. Rodriguez, H. Yu, J. Penner, and S. Strahan (2009),
429 Sensitivity of aerosol optical thickness and aerosol direct radiative effect to
430 relative humidity. *Atmos. Chem. Phys.*, 9, 2375 – 2386, doi:10.5194/acp-9-
431 2375-2009.
- 432Chin, M., P. Ginoux, S. Kinne, O. Torres, B. Holben, B.N. Duncan, R.V. Martin, J.
433 Logan, A. Higurashi, T. Nakajima (2002), Tropospheric aerosol optical
434 thickness from the GOCART model and comparisons with satellite and sun
435 photometer measurements. *J. Atmos. Phys.* 59, 461–483, doi:
436 [http://dx.doi.org/10.1175/1520-0469\(2002\)059](http://dx.doi.org/10.1175/1520-0469(2002)059).
- 437Colarco, P., A. da Silva, M. Chin, and T. Diehl (2010), Online simulations of global
438 aerosol distributions in the NASA GEOS-4 model and comparisons to
439 satellite and ground-based aerosol optical depth. *J. Geophys. Res.*, 115,
440 D14207, doi:10.1029/2009JD012820.
- 441Darmenov, A., and A.M. da Silva (2013), The quick fire emissions dataset (QFED)
442 - Documentation of versions 2.1, 2.2 and 2.4. NASA Technical Report Series
443 on Global Modeling and Data Assimilation. NASA TM-[2013-104606](#), 32,
444 183p.
- 445Dee, D.P., L. Rukhovets, R. Todling, A.M. da Silva, and J.W. Larson (2001), An
446 Adaptive Buddy Check for Observational Quality Control. *Quarterly Journal*
447 *of the Royal Meteorological Society*, 127(577), 2451–2471,
448 doi:10.1002/qj.49712757714.
- 449Dee, D.P., and A.M. da Silva (1999), Maximum-Likelihood Estimation of Forecast
450 and Observation Error Covariance Parameters. Part I: Methodology. *Mon.*
451 *Weather Rev.*, 127(8), 1822–1834, doi:<http://dx.doi.org/10.1175/1520-0493>.

- 452 Derber, J. C., R.J. Purser, W.-S. Wu, R. Treadon, M. Pondeva, D. Parrish, and D.
453 Kleist (2003), Flow-dependent Jb in a global grid-point 3D-Var. *Proc.*
454 *ECMWF annual seminar on recent developments in data assimilation for*
455 *atmosphere and ocean*. Reading, UK, 8-12 Sept. 2003.
- 456 Dey, S., and L. Di Girolamo (2011), A decade of change in aerosol properties over
457 the Indian subcontinent, *Geophys. Res. Lett.*, 38, L14811,
458 doi:10.1029/2011GL048153.
- 459 Di Girolamo, L., T.C. Bond, D. Bramer, D.J. Diner, F. Fettinger, R.A. Kahn, J.V.
460 Matronchik, M.V. Ramanathan, and P.J. Rash (2004), Analysis of Multi-angle
461 Imaging SpectroRadiometer (MISR) aerosol optical depths over greater India
462 during winter 2001 – 2004. *Geophys. Res. Lett.*, 31, L23115,
463 doi:10.1029/2004GL021273.
- 464 Dunion, J. P., and C. S. Velden (2004), The impact of the Saharan air layer on
465 Atlantic tropical cyclone activity, *Bull. Am. Meteorol. Soc.*, 85(3), 353– 365,
466 doi:10.1175/BAMS-85-3-353.
- 467 Fasullo, J., and K. Trenberth (2012). A less cloudy future: the role of subtropical
468 subsidence in climate sensitivity, *Science*, 338, 792-794.
- 469 Ganguly, D., A. Jayaraman, and H. Gadhavi (2005), In situ ship cruise
470 measurements of mass concentration and size distribution of aerosols over
471 Bay of Bengal and their radiative impacts. *J. Geophys. Res.*, 110, D06205,
472 doi:10.1029/2004JD005325.
- 473 Hill, C, C. DeLuca, Balaji, M. Suarez, and A. da Silva (2004): The architecture of
474 the Earth System Modeling Framework. *Computing in Science and*
475 *Engineering*, 6(1), 18–28.

- 476Hsu, N.C., R. Gautam, A.M. Sayer, C. Bettenhausen, C. Li, M.J. Jeong, S.C. Tsay,
477 and B.N. Holben (2012), Global and regional trends of aerosol optical depth
478 over land and ocean using SeaWiFS measurements from 1997 to 2010.
479 *Atmos. Chem. Phys. Discuss.*, 12, 8465-8501, doi:10.5194/acpd-12-8465-
480 2012.
- 481Huffman, G.J., R.F. Adler, D.T. Bolvin, G. Gu, E.J. Nelkin, K.P. Bowman, Y.
482 Hong, E.F. Stocker, D.B. Wolff (2007), The TRMM multisatellite
483 precipitation analysis (TMPA): quasi-global, multiyear, combined-sensor
484 precipitation estimates at fine scales. *J. Hydrometeorology*, 8, 38 – 55, doi:
485 10.1175/JHM560.1.
- 486Kaskaoutis, D.G., S.K. Kharol, P.R. Sinha, R.P. Singh, K.V.S. Badarinath, W.
487 Mehdi, and M. Sharma (2011a). Contrasting aerosol trends over South Asia
488 during the last decade based on MODIS observations. *Atmos. Meas. Tech.*
489 *Discuss.*, 4, 5275–5323, doi:10.5194/amtd-4-5275-2011.
- 490Kaskaoutis, D.G., S. Kumar Kharol, P.R. Sinha, R.P. Singh, H.D. Kambezidis, A.
491 Rani Sharma, and K.V.S. Badarinath (2011b), Extremely large anthropogenic
492 aerosol contribution to total aerosol load over the Bay of Bengal during winter
493 season. *Atmos. Chem. Phys.*, 11, 7097–10 7117, doi:10.5194/acp-11-7097-
494 2011.
- 495Kishcha, P., B. Starobinets, O. Kalashnikova, and P. Alpert (2011), Aerosol optical
496 thickness trends and population growth in the Indian subcontinent. *Int. J.*
497 *Remote. Sens.*, 32, 9137-9149, doi:10.1080/01431161.2010.550333.
- 498Kishcha, P., B. Starobinets, C.N. Long, P. Alpert (2012), Unexpected increasing
499 AOT trends over north-west Bay of Bengal in the early post-monsoon season.
500 *J. Geophys. Res.*, 117, D23208, doi 10.1029/2012JD018726.

- 501 Krishna Moorthy, K., S. Suresh Babu, M.R. Manoj, and S.K. Satheesh (2013),
502 Buildup of aerosols over the Indian region. *Geophys. Res. Lett.*,
503 doi:10.1002/GRL.50165.
- 504 Kumar, A., M.M. Sarin, and B. Srinivas (2010), Aerosol iron solubility over Bay of
505 Bengal: Role of anthropogenic sources and chemical processing, *Marine*
506 *Chemistry*, 121, 167–175.
- 507 Lary, D.J., L.A. Remer, D. MacNeill, B. Roscoe, and S. Paradise (2009), Machine
508 Learning and Bias Correction of MODIS Aerosol Optical Depth. *Geoscience*
509 *and Remote Sensing Letters*, IEEE, 6(4), 694–698, doi:
510 [10.1109/LGRS.2009.2023605](https://doi.org/10.1109/LGRS.2009.2023605).
- 511 Mishchenko, M. I., and I. V. Geogdzhayev (2007), Satellite remote sensing reveals
512 regional tropospheric aerosol trends, *Opt. Express*, 15, 7423 – 7438,
513 doi:10.1364/OE.15.007423.
- 514 Moorthy, K.K., S.K. Satheesh, S.S. Babu, and C.B.S. Dutt (2008), Integrated
515 campaign for aerosols, gases and radiation budget (ICARB): An overview. *J.*
516 *Earth Syst. Sci.*, 117, 243–262, doi:[10.1007/s12040-008-0029-7](https://doi.org/10.1007/s12040-008-0029-7).
- 517 Pawson, S., R.S. Stolarski, A.R. Douglass, P.A. Newman, J.E. Nielsen, S.M. Frith,
518 and M.L. Gupta (2008), Goddard Earth Observing System Chemistry-Climate
519 Model Simulations of Stratospheric Ozone-Temperature Coupling Between
520 1950 and 2005. *J. Geophys. Res.*, 113(D12), D12103,
521 doi:10.1029/2007JD009511.
- 522 Prasad, A.K. and R.P. Singh (2007), Comparison of MISR-MODIS aerosol optical
523 depth over the Indo-Gangetic basin during the winter and summer seasons
524 (2000-2005). *Remote Sensing of Environment*, 107, 109 – 119,
525 doi:10.1016/j.rse.2006.09.026.

- 526 Ramachandran, S. and A. Jayaraman (2003), Spectral aerosol optical depths over
527 Bay of Bengal and Chennai: II – Sources, anthropogenic influence and model
528 estimates. *Atmos. Env.*, 37, 1951–1962, doi:[10.1016/S1352-2310\(03\)00082-7](https://doi.org/10.1016/S1352-2310(03)00082-7).
- 529 Ramanathan, V., and M. Ramana (2005), Persistent, widespread and strongly
530 absorbing haze over the Himalayan foothills and the Indo-Gangetic plains.
531 *Pure and Applied Geophysics*, 162, 1609 – 1626, doi:10.1007/s00024-005-
532 2685-8.
- 533 Razali, N.M., and Y.B. Wah (2011), Power comparisons of Shapiro-Wilks,
534 Kolmogorov-Smirnov, Lilliefors and Anderson-Darling tests. *J. Statistical*
535 *Modeling and Analytics*, 2, 21-33.
- 536 Rienecker, M.M., M.J. Suarez, R. Todling, J. Bacmeister, L. Takacs, H-C Liu, W Gu,
537 M. Sienkiewicz, R.D. Koster, R. Gelaro, I. Stajner, and E. Nielsen (2008),
538 The GEOS-5 Data Assimilation System--Documentation of Version 5.0.1,
539 5.1.0, and 5.2.0. NASA/TM-2007-104606, 27, 1-118.
- 540 Rienecker, M.M., and Co-authors (2011), MERRA: NASA's Modern-Era
541 Retrospective Analysis for Research and Applications. *J. Climate*, 24, 3624–
542 3648. doi:<http://dx.doi.org/10.1175/JCLI-D-11-00015.1>
- 543 Rienecker, M.M., M.J. Suarez, R. Gelaro, R. Todling, J. Bacmeister, E. Liu, M.G.
544 Bosilovich, S.D. Schubert, L. Takacs, G.-K. Kim, S. Bloom, J. Chen, D.
545 Collins, A. Conaty, A. da Silva, et al. (2011), MERRA: NASA's Modern-Era
546 Retrospective Analysis for Research and Applications. *J. Climate*, 24, 3624-
547 3648, doi: 10.1175/JCLI-D-11-00015.1.
- 548 Shapiro, S.S., and M.B. [Wilk](#) (1965), An analysis of variance test for normality
549 (complete samples). *Biometrika*, 52, 591 – 611, doi:[10.1093/biomet/52.3-](https://doi.org/10.1093/biomet/52.3-4.591)
550 [4.591](https://doi.org/10.1093/biomet/52.3-4.591).

- 551 Sharma, A.R., S.K. Kharol, K.V.S. Badarinath, and D. Singh (2010), Impact of
552 agriculture crop residue burning on atmospheric aerosol loading – a study
553 over Punjab State, India, *Ann. Geophys.*, 28, 367–379, doi:10.5194/angeo-28-
554 367-2010.
- 555 Tripathi, S.N., S. Day, A. Chandell, S. Srivastava, R.P. Singh, and B. Holben
556 (2005), Comparison of MODIS and AERONET derived aerosol optical depth
557 over the Ganga basin, India. *Ann. Geophys.*, 23, 1093-1101,
558 doi:10.5194/angeo-23-1093-2005.
- 559 U.S. Census Bureau <http://www.census.gov/ipc/www/idb/>
- 560 Venkataraman, C., G. Habib, D. Kadamba, M. Shrivastava, J.-F., Leon, B.
561 Crouzille, O. Boucher, D. Streets (2006), Emissions from open biomass
562 burning in India: Integrating the inventory approach with high-resolution
563 Moderate Resolution Imaging Spectroradiometer (MODIS) active-fire and
564 land cover data. *Global Biogeochem. Cycles*, 20, GB2013,
565 doi:10.1029/2005GB002547.
- 566 Vinoj, V., S.S. Babu, S.K. Satheesh, K.K. Moorthy, and Y.J. Kaufman (2004),
567 Radiative forcing by aerosols over the Bay of Bengal region derived from
568 shipborne, island-based, and satellite (Moderate-Resolution Imaging
569 Spectroradiometer) observations. *J. Geophys. Res.*, 109, D05203,
570 doi:10.1029/2003JD004329.
- 571 Wu, W.S., R.J. Purser, and D.F. Parrish (2002): Three-dimensional variational
572 analysis with spatially inhomogeneous covariances. *Mon. Weather. Rev.*, 130,
573 2905–2916, doi:<http://dx.doi.org/10.1175/1520-0493>.

- 574Zhang, J. and J.S. Reid (2006), MODIS Aerosol Product Analysis for Data
575 Assimilation: Assessment of Over-Ocean Level 2 Aerosol Optical Thickness
576 Retrievals. *J. Geophys. Res.*, 111(D22), D22207. doi:10.1029/2005JD006898.
- 577Zhang, J.L. and J.S. Reid (2010), A decadal regional and global trend analysis of
578 the aerosol optical depth using a data-assimilation grade over-water MODIS
579 and Level 2 MISR aerosol products. *Atmos. Chem. Phys.*, 10, 10949-10963,
580 doi:10.5194/acp-10-10949-2010.
- 581Zhao, T. X.-P., I. Laszlo, W. Guo, A. Heidinger, C. Cao, A. Jelenak, D. Tarpley,
582 and J. Sullivan (2008), Study of long-term trend in aerosol optical thickness
583 observed from operational AVHRR satellite instrument, *J. Geophys. Res.*,
584 113, D07201, doi:10.1029/2007JD009061.

585

586**Acknowledgements** We gratefully acknowledge the GES-DISC Interactive Online
587Visualization and Analysis Infrastructure (Giovanni) for providing us with TRMM data.

588

589Table 1. The overview of main attributes of NASA MERRAero assimilated aerosol
590data.

Feature	Description
Model	GEOS-5 Earth Modeling System (with GOCART aerosol components); Constrained by MERRA Meteorology (Replay) Land sees obs. precipitation (like MERRALand) Driven by QFED daily Biomass Emissions
Aerosol data assimilation	Local Displacement Ensembles (LDE) MODIS reflectances AERONET Calibrated AOT's (Neural Net) Stringent cloud screening
Period	mid 2002-present (Aqua + Terra)
Resolution	Horizontal: nominally 50 km Vertical: 72 layers, top ~85 km
Aerosol Species	Dust, sea-salt, sulfates, organic & black carbon

591

592

593

594 Table 2. Eight-year (2002-2009) mean AOT (τ), standard deviation (sd), and AOT slope
 595 (α) of MERRAero AOT averaged over the specified zones in October^a.

596

Area	Zone #	Geographic Coordinates	τ	sd	α (per year)	S – W test	p
IS	1	28.5N – 31.5N 72.7E – 75.7E	0.53	0.07	-0.005	Normal	Not significant
	2	27N – 30N 75.7E – 78.7E	0.50	0.08	-0.004	Normal	Not significant
	3	25N – 28N 78.7E – 81.7E	0.51	0.08	0.008	Normal	Not significant
	4	24N – 27N 82.5E – 85.5E	0.43	0.05	0.012	Normal	Not significant
	5	22N – 25N 86E – 89E	0.35	0.05	0.010	Normal	Not significant
BoB	6	18N – 21N 87E – 90E	0.22	0.05	0.015	Normal	0.043
	7	15N – 18N 84E – 87E	0.20	0.05	0.020	Normal	0.006

597

598^aThe decision based on the Shapiro – Wilk normality test for residuals (S-W test) and
 599 the significance level (p) are also displayed. If the p value was too high as compared
 600 with the 0.05 significance level, the obtained linear fit was considered as statistically
 601 insignificant.

602Table 3. The eight-year mean AOT (τ), standard deviation (sd), and AOT slope (α) for
 603long-term changes of MERRAero AOT for different aerosol species (desert dust;
 604organic and black carbon; and sulfates) averaged over specified zones in October. F
 605corresponds to the fraction of aerosol component AOT (in percentages) from the total
 606MERRAero AOT.

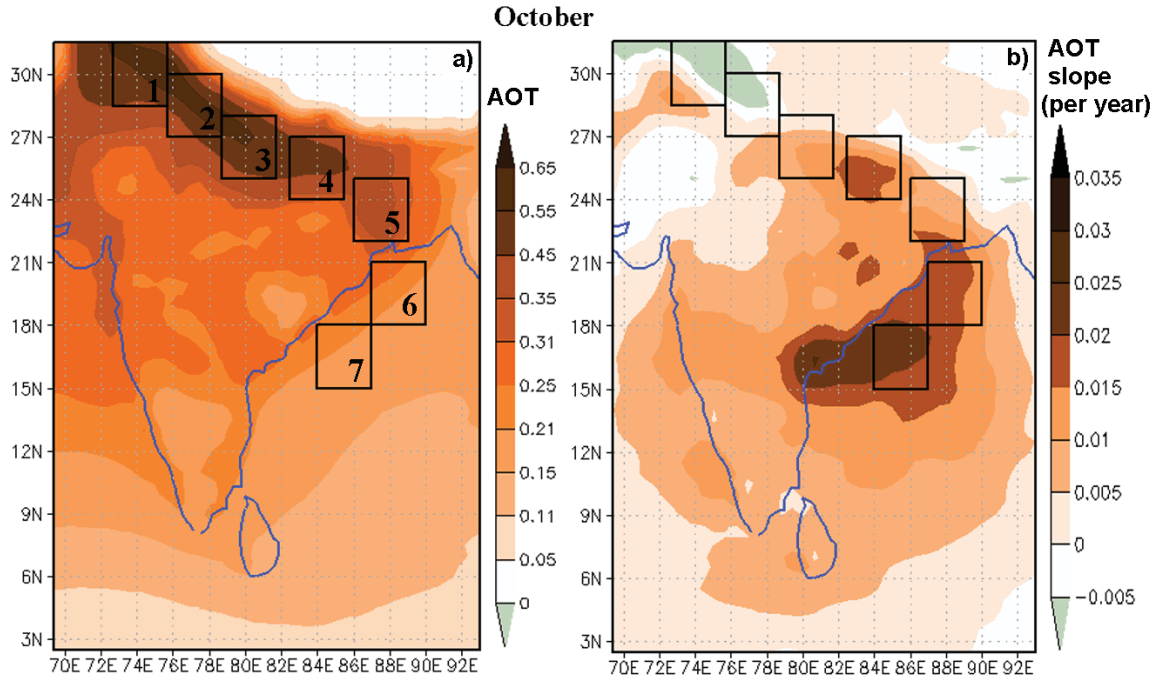
607

Area	Zone #	F %	τ	sd	α (per year)	S – W test	p
					Sulfates		
IS	1	31.7	0.17	0.04	0.001	Normal	Not significant
	2	36.7	0.18	0.04	-0.001	Normal	Not significant
	3	43.7	0.22	0.05	0.004	Normal	Not significant
	4	49.7	0.22	0.04	0.006	Normal	Not significant
	5	55.9	0.20	0.03	0.004	Normal	Not significant
BoB	6	52.9	0.12	0.03	0.008	Normal	0.050
	7	50.7	0.10	0.03	0.011	Normal	0.004
					Organic and black carbon		
IS	1	37.7	0.20	0.05	-0.011	Normal	Not significant
	2	39.2	0.20	0.03	-0.009	Normal	Not significant
	3	37.7	0.19	0.02	-0.001	Normal	Not significant
	4	37.5	0.16	0.02	0.002	Normal	Not significant
	5	34.9	0.12	0.02	0.003	Normal	Not significant
BoB	6	28.8	0.06	0.02	0.004	Normal	Not significant
	7	25.9	0.05	0.02	0.005	Normal	0.026
					Desert dust		
IS	1	29.5	0.16	0.04	0.006	Normal	Not significant
	2	23.2	0.12	0.03	0.006	Normal	Not significant
	3	17.8	0.09	0.03	0.005	Normal	Not significant
	4	12.2	0.05	0.02	0.004	Normal	Not significant
	5	8.0	0.03	0.01	0.004	Normal	0.035
BoB	6	8.3	0.02	0.01	0.004	Normal	0.012
	7	8.1	0.02	0.01	0.004	Normal	0.008

608

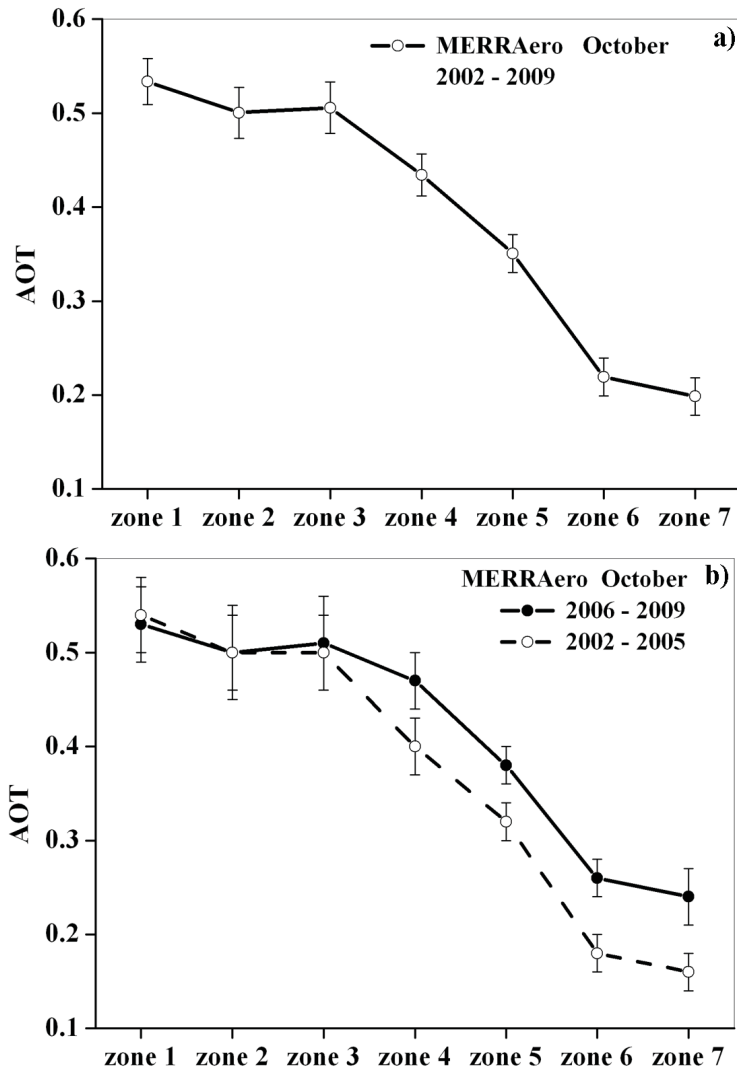
609

610



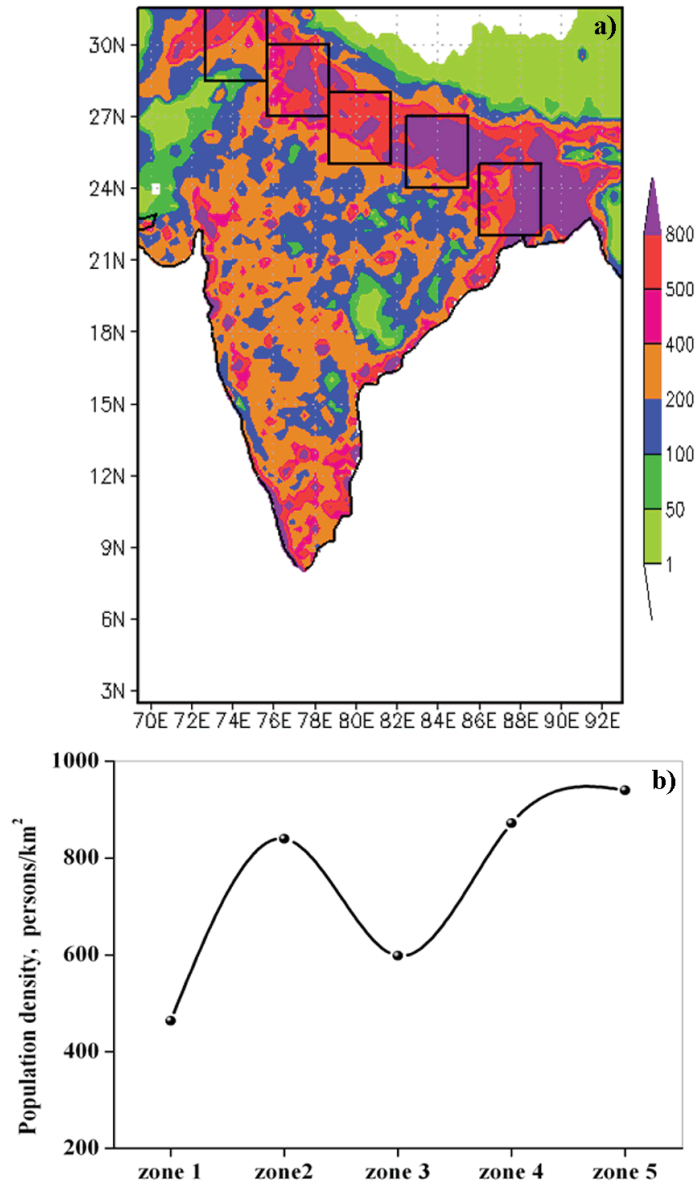
612Figure 1. Spatial distributions of (a) the eight year (2002 – 2009) mean MERRAero
613AOT and (b) its trends (characterized by AOT slopes) in October. The AOT trend
614values correspond to the slope of the linear regression analysis. The squares show the
615locations of zones 1 to 7 within the study region.

616



617Figure 2. a - zone-to-zone variations of eight-year (2002-2009) mean MERRAero AOT
 618averaged over the specified zones. b - zone-to-zone variations of MERRAero AOT
 619averaged over the first four-year (2002-2005) period and over the second four-year
 620(2006-2009) period. The error bars show the standard error of mean AOT.

621

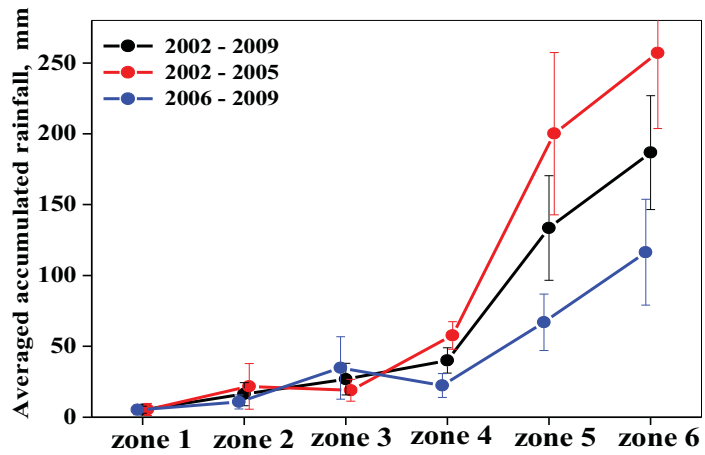


623 Figure 3. a – population density (persons km⁻²) distributions over the Indian
 624 subcontinent. b – zone-to-zone variations of population density averaged over the
 625 specified zones. The GPW-v3 gridded population density data for the year 2005 were
 626 used (<http://sedac.ciesin.columbia.edu/data/collection/gpw-v3>).

627

628

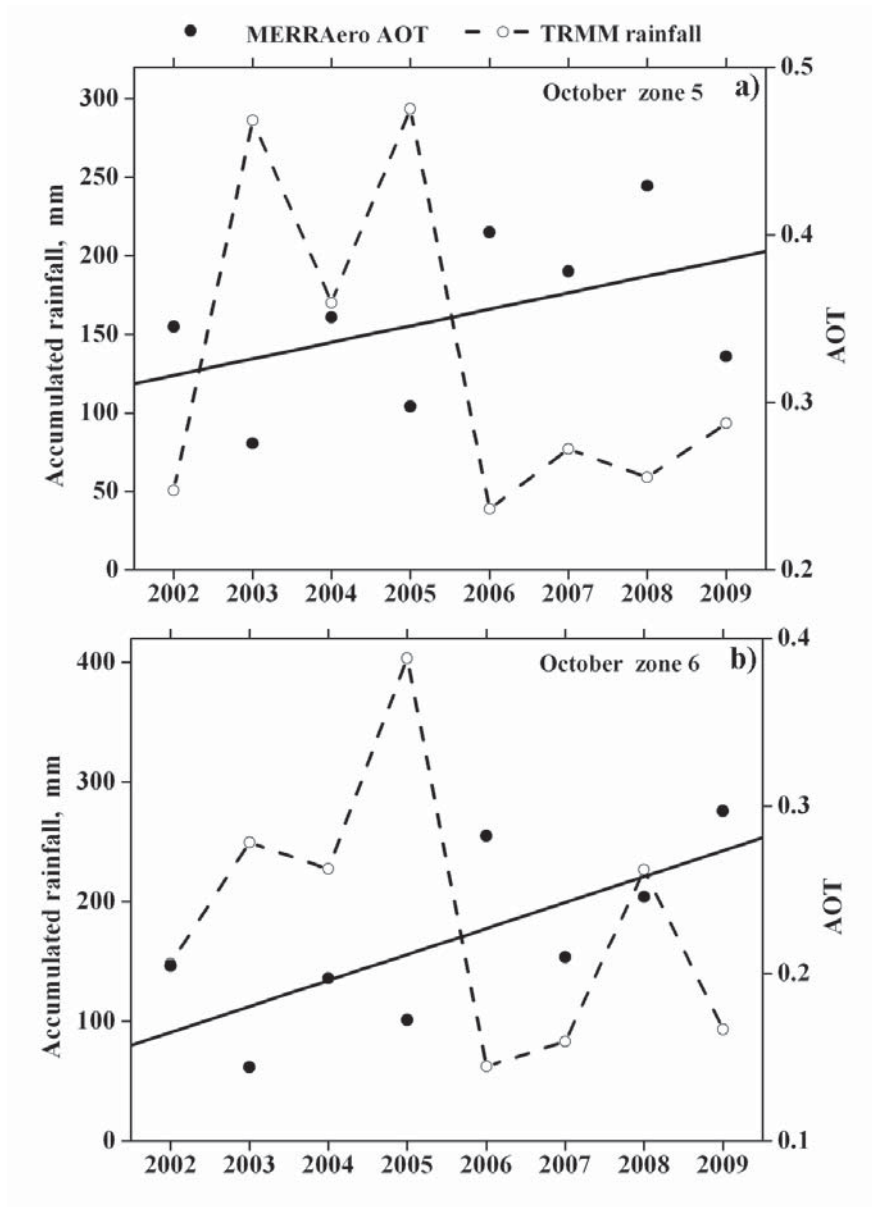
629



630Figure 4. Zone-to-zone variations of TRMM accumulated rainfall over the specified
 631zones in October averaged over the eight-year study period (2002 – 2009), over the first
 6324-year period (2002 – 2005), and over the second 4-year period (2002 – 2009). The
 633error bars show the standard error of mean accumulated rainfall. TRMM data from the
 6343B42V6 archive were used.

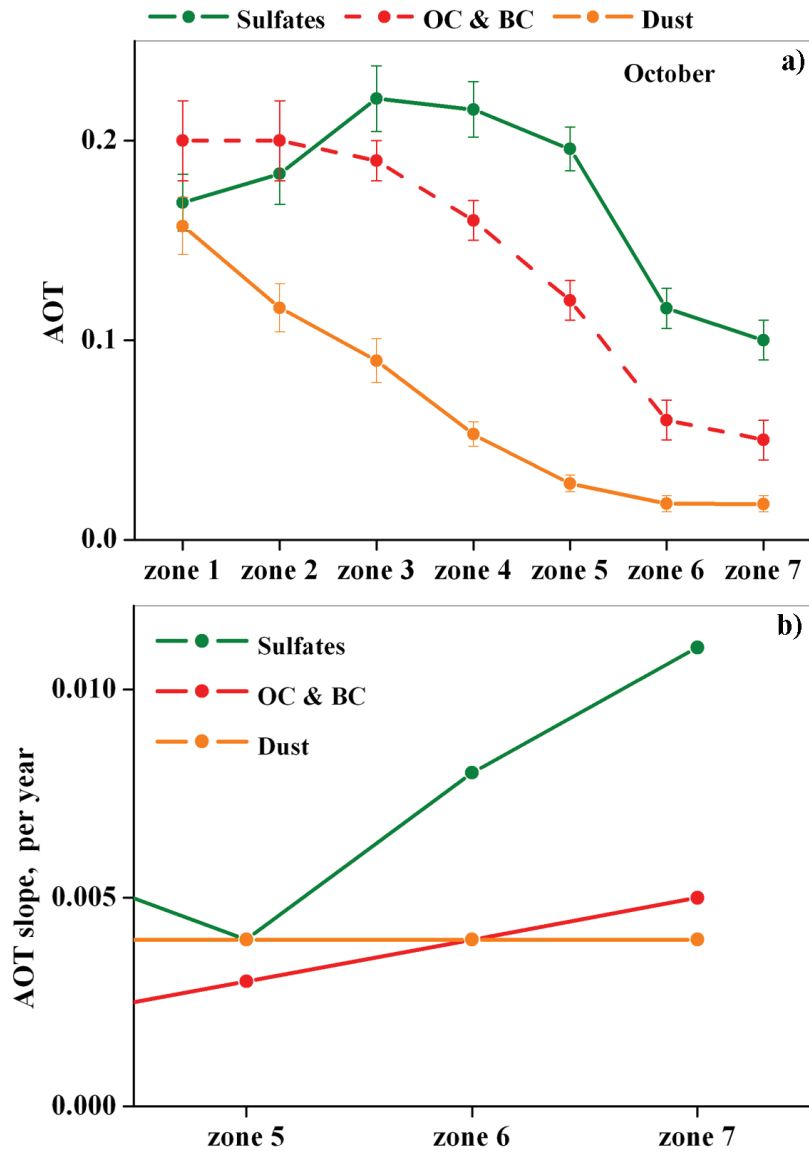
635

636

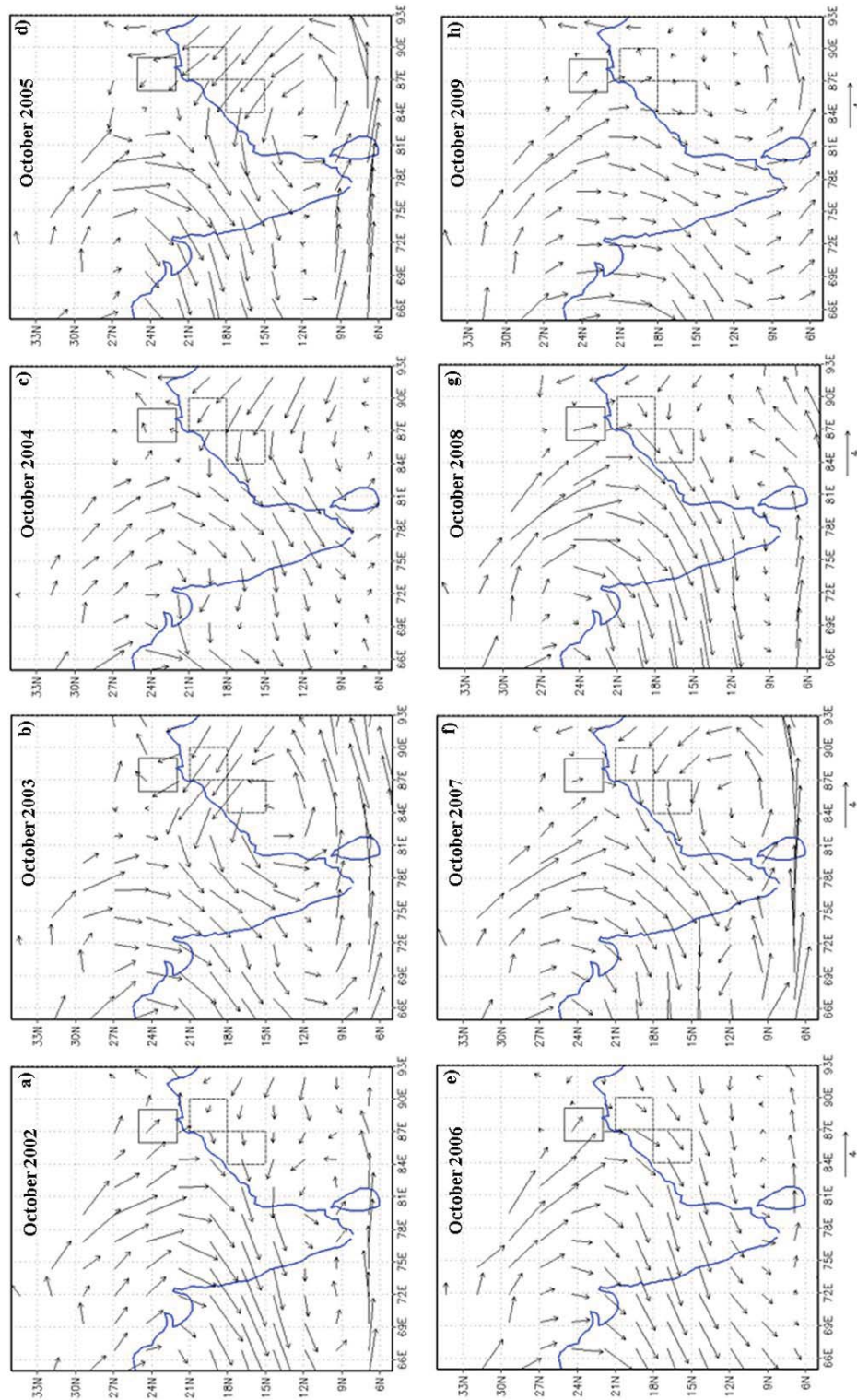


637 Fig. 5. Year-to-year variations of MERRAero AOT and TRMM rainfall over (a) the east
 638 of the Ganges basin (zone 5) and (b) north-west BoB (zone 6) in each October during
 639 the study period. TRMM rainfall data from the 3B42V6 archive were used. The straight
 640 solid lines designate linear fits.

641

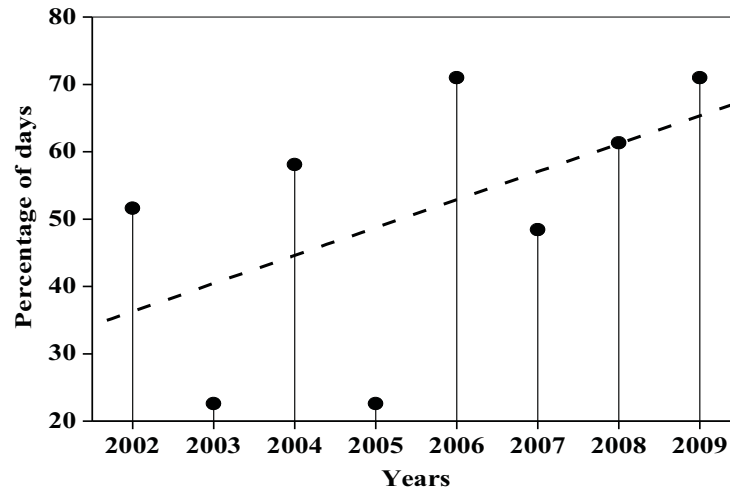


642Figure 6. Zone-to-zone variations of (a) eight-year (2002-2009) mean MERRA AOT of
 643different aerosol components (sulfates (SU), organic and black carbon (OC & BC), and
 644desert dust) averaged over the specified zones in October, and (b) their AOT trends
 645(characterized by the slope of the linear regression analysis). The error bars show the
 646standard error of mean AOT.



648Figure 7. Spatial distributions of mean MERRA wind vectors of the 700-850 hPa layer 649in each October during the study period.

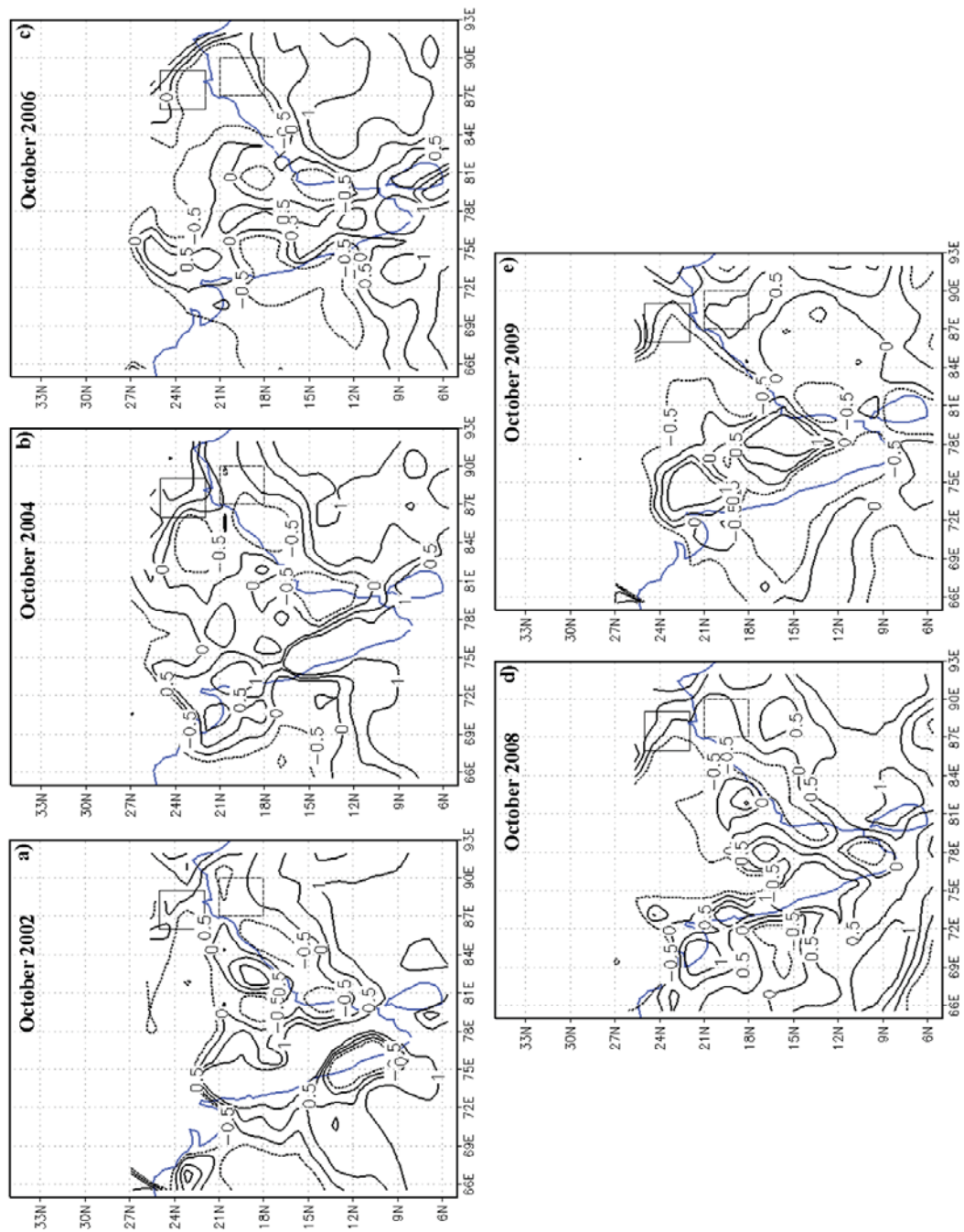
650



651 Figure 8. Numbers of days (in percentage form) in each October during the study period
652 when prevailing wind (transporting air pollution) blew from the east of the Ganges
653 basin (zone 5) to north-west BoB (zone 6). The straight dashed line designates a linear
654 fit.

655

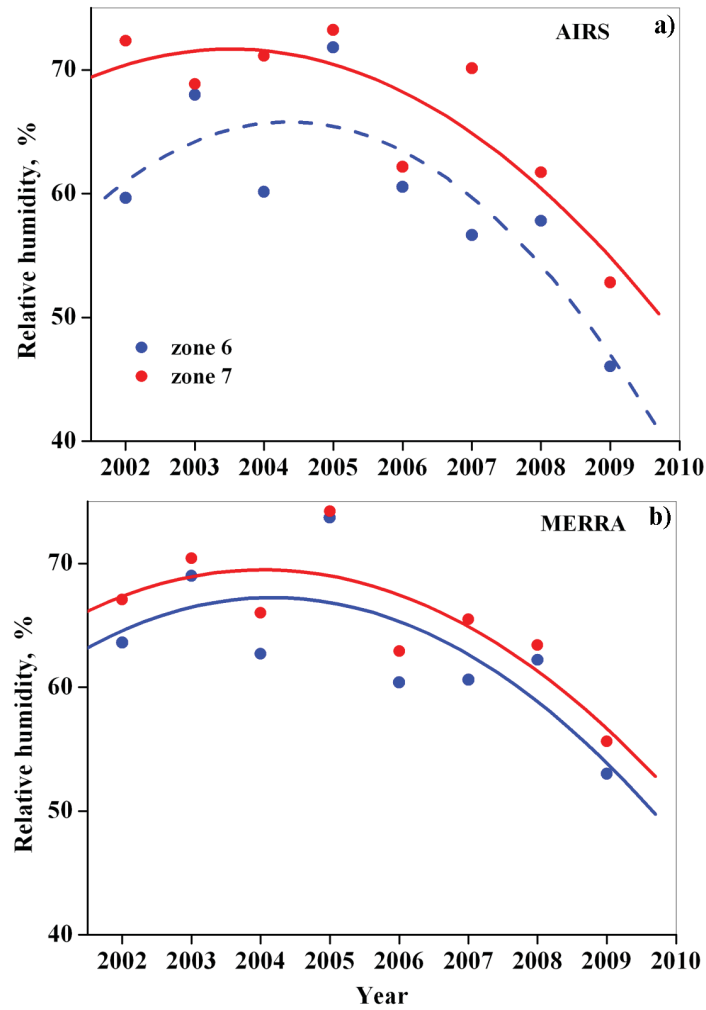
656



657Figure 9. Spatial distributions of mean wind convergence (10^{-6} s^{-1}) of the 700-850 hPa
 658layer for each October, when the number of days with prevailing winds, blowing from
 659the east of the Ganges basin (zone 5) to north-west BoB (zone 6), exceeded 50%.
 660MERRA wind reanalysis data were used.

661

662

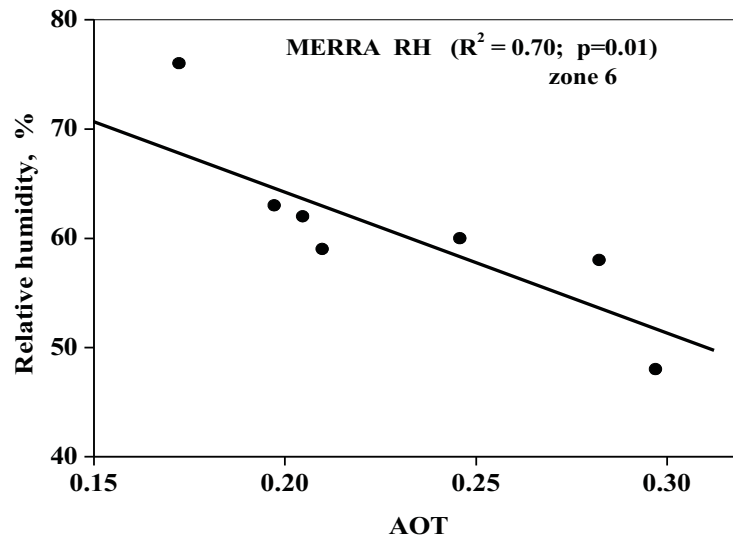


663Figure 10. Year-to-year variations of relative humidity (RH) of the 700-850 hPa layer in
 664each October during the study period based on (a) AIRS monthly data (taken on the
 665descending node of the orbit, on the day side of the Earth), and (b) the MERRA
 666monthly data.

667

668

669



670Figure 11. Scatter-plot between monthly MERRA relative humidity of the 700-850 hPa
671layer and MERRAero AOT over north-west BoB (zone 6) in each October during the
672study period. The straight line designates a linear fit.

673